

Kinematics and activity of M dwarfs in LAMOST DR1 *

Zhen-Ping Yi^{1,2,3}, A-Li Luo¹, Jing-Kun Zhao¹, Yi-Han Song¹, Jing-Chang Pan²,
Yong-Heng Zhao¹ and Yong Zhang⁴

¹ Key Laboratory of Optical Astronomy, National Astronomical Observatories, Chinese Academy of Sciences, Beijing 100012, China; *lal@nao.cas.cn*

² Shandong University, Weihai 264209, China

³ University of Chinese Academy of Sciences, Beijing 100049, China

⁴ Nanjing Institute of Astronomical Optics & Technology, National Astronomical Observatories, Chinese Academy of Sciences, Nanjing 210042, China

Received 2014 September 7; accepted 2014 October 30

Abstract We report on the first investigation into kinematics and chromospheric activity of M dwarfs from the Guo Shou Jing Telescope (also called the Large Sky Area Multi-Object Fiber Spectroscopic Telescope – LAMOST) data release one (DR1). The sample comprises 71 304 M dwarfs. Their fundamental parameters such as spectral types, radial velocities, important molecular band indices and magnetic activities are measured. Their distances are determined by a spectroscopic parallax relation. Space motion (U , V , W) and Galactocentric cylindrical coordinates (R , θ , Z) for the M dwarfs are also computed. We examine velocity dispersion as a function of height from the Galactic plane and find that all three components of velocity dispersion increase with height as measured with respect to the Galactic plane. The investigation into chromospheric activities along the height from the Galactic plane confirms that M dwarfs closer to the Galactic plane are more likely to be active. We take a pure kinematical approach to select thin disk stars and thick disk stars from our sample, then to investigate the differences in properties between these two populations. Our analysis is in excellent agreement with previous studies and leads to a better understanding of the structure of the Galactic disk.

Key words: stars: kinematics — stars: magnetic fields — stars: low-mass, brown dwarfs — stars: fundamental parameters

1 INTRODUCTION

Kinematic studies of M dwarfs can reveal the origin and ages of M dwarfs and thus provide insights into the evolution of the Galaxy. Many studies have investigated kinematics of low-mass stars based on hundreds of spectral samples and derived the velocity dispersions in U , V and W (Wielen 1977; Ratnatunga & Uggren 1997; Vyssotsky 1956; Reid et al. 1995; Reid et al. 2002; Bochanski et al. 2005). Bochanski et al. (Bochanski et al. 2007) enlarged the sample size to $\sim 7\,000$ M dwarfs by using data from the Sloan Digital Sky Survey (SDSS) (York et al. 2000) and investigated the difference

* Supported by the National Natural Science Foundation of China.

in velocity dispersions between the thin disk and the thick disk. Magnetic activity is another notable feature of M dwarfs. In recent years, many studies have examined this feature (Gizis et al. 2002; West et al. 2004; West et al. 2008; West et al. 2011). These studies indicated that magnetic activity varies with the spectral type and the age of M dwarfs. However, the mechanism behind magnetic field production remains an unsolved problem.

Recently, with the advent of the large sky survey ability of the Guo Shou Jing Telescope (also named the Large Sky Area Multi-Object Fiber Spectroscopic Telescope – LAMOST) (Cui et al. 2012; Zhao et al. 2012), there are many more stars available for analysis than ever before, allowing for a detailed examination of the local Galactic disk with large spectral samples. LAMOST, also known as Wang-Su Reflecting Schmidt Telescope, is a new type of wide field telescope with a large aperture, which can acquire several tens of thousands of spectra per night. The data set contained in LAMOST data release one (DR1), including spectra from the pilot survey and spectra from the first year of the regular spectroscopic survey, has already been published. In LAMOST DR1, there are 113 741 M-type stellar spectra, of which 58 360 spectra are from the pilot survey and 55 381 are from the regular survey. With these M dwarfs, we investigate the kinematics and chromospheric activity of M dwarfs. We measure fundamental parameters including spectral type, radial velocity, the equivalent width of the $H\alpha$ emission line and important molecular band indices from the spectra. Combined with proper motions from PPMXL (Roesser et al. 2010), radial velocities and distances, we compute space motions of M dwarfs to examine observed distributions of kinematic quantities. We also compute the activity fraction of M dwarfs as a function of the height from the Galactic plane and try to examine the link between the activity and age.

The paper is organized as follows. In Section 2, we describe the spectra observed by LAMOST and selection of the sample of M dwarfs. Section 3 describes the derivation of parameters including spectral types, radial velocities, distances and space motions. Our results are summarized and discussed in Section 4.

2 DATA AND SAMPLE SELECTION

The resolution of LAMOST spectra is $R = 1800$ over a wavelength coverage of 3690 – 9100 Å. The two arms of each spectrograph cover the entire wavelength range with 200 Å of overlap. The wavelength coverage of the blue end is 3690 – 5900 Å while that of the red end is 5700 – 9100 Å. The raw data have been reduced with the LAMOST 2D and 1D pipelines, including bias subtraction, cosmic-ray removal, spectral trace and extraction, flat-fielding, wavelength calibration, sky subtraction and classification. The LAMOST 1D pipeline approximately classifies observed spectra by using chi-square fitting (Luo et al. 2012). We select out the spectra classified as M type using the 1D pipeline and visually inspect them by using the Hammer spectral typing facility (Covey et al. 2007). After excluding spectroscopic binaries and bad spectra through visual inspection, 113 741 M-type spectra remain. However, in this spectral set there are spectra that are observed repeatedly. For spectra from the same star, we keep the one with the highest signal to noise ratio (S/N) and exclude the rest. After excluding spectra observed repeatedly, 102 153 spectra are left.

In the M dwarf catalog of the LAMOST pilot survey, it is estimated that M giant contamination is less than 4% by color $J - H$ (Yi et al. 2014). In order to get a cleaner M dwarf sample, we make a more detailed investigation on M giant identification from M dwarfs. Compared to M dwarfs, M giants are redder in color. It is also known that M giants exhibit different spectral morphology near TiO and CaH bandheads. We plot spectral indices CaH2 + CaH3 against TiO5 in Figure 1. There is an obvious gap along the red line, and points above the line might be giants (Zhong et al. in prep). We also examine the $J - H$ and $J - K_s$ colors of the points above the gap using their JHK_s magnitudes, which are derived by cross-matching our sample with the near-infrared 2MASS catalog (Skrutskie et al. 2006). It turns out that about 60% of the points above the red line meet $J - H > 0.8$ and $J - K_s > 1$ (Bessell & Brett 1988). This indicates that the CaH vs TiO5 relation is rather effective

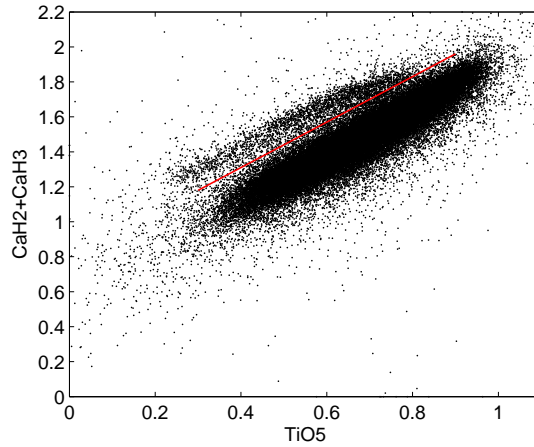


Fig. 1 CaH vs. TiO5 in LAMOST M-type stellar spectra.

in distinguishing M giants from M dwarfs. The stars meeting both criteria are selected as M giant candidates and there are 2298 of them. We exclude these giant candidates, leaving 99 855 objects in our final sample.

3 PARAMETER MEASUREMENTS

Spectral types of M dwarfs in our sample are derived using the modified Hammer code (Yi et al. 2014) and are then confirmed by visual inspection. Radial velocities of M dwarfs have been measured by the cross correlation method. We also measure the magnetic activity traced by the $H\alpha$ emission line, a number of prominent molecular band indices, and the metal-sensitive parameter ζ . These measurement methods were described in Yi et al. (2014).

Distances to the M dwarfs in our sample are determined by using spectroscopic parallax. The distance equation is:

$$m_\lambda - M_\lambda = 5 \log d - 5 - A_\lambda,$$

where d is the distance, m_λ is the apparent magnitude in a certain filter, M_λ is the absolute magnitude of the same filter and needs to be measured before the distance computation, and A_λ is the extinction of the same filter.

We compute M_J of M dwarfs using M_J -spectral type relations derived by Hawley et al. (2002). The relations that we adopted are listed below:

$$\begin{aligned} M_J &= 6.46 + 0.26 \text{ SPT}, & 0 \leq \text{SPT} \leq 3, \\ M_J &= 8.34, & \text{SPT} = 4, \\ M_J &= 5.73 + 0.74 \text{ SPT}, & 5 \leq \text{SPT} \leq 7, \\ M_J &= 8.83 + 0.29 \text{ SPT}, & 8 \leq \text{SPT} \leq 9, \end{aligned}$$

where SPT is 0 – 9 corresponding to the spectral types M0–M9 and J is 2MASS magnitude.

We estimate the reddening effect of our stars in J magnitude. Stars are divided into the GAC group ($\sim 1/3$ of the sample) and the notGAC group ($\sim 2/3$ of the sample) (GAC means the stars are in the direction of the Galactic anticenter with low galactic latitude, while notGAC means the stars are not in the direction of the Galactic anticenter with higher galactic latitude). For the notGAC group, we compute the extinction for the total column along the line of sight using the extinction maps

of Schlegel et al. (1998), with the updated coefficients from Schlafly & Finkbeiner (2011). For the GAC group, we compute the extinction using the three dimensional extinction map of the Galactic anticenter (Chen et al. 2014). We estimate the distance scale of our sample and get a maximum distance of 800 pc (for an M0 star with apparent magnitude $m_v = 18$, the absolute magnitude is adopted to be $M_v = 8.7$). For the notGAC group, the average extinction in J is 0.025 mag, while for the GAC group, the average extinction at the distance of 900 pc is 0.09 mag in J . Actually, about 90% of our stars are closer than 400 pc, thus for each group, the real average extinction should be smaller than the corresponding extinction value that we derived above. Therefore, we neglect the reddening corrections when computing the distance to stars in our sample.

We match our sample with the PPMXL catalog to obtain the proper motions. To reduce the systematic shift from zero in the PPMXL survey, Carlin et al. (2013) derived new corrections to the proper motions using $\sim 110\,000$ QSOs and galaxies. We use the polynomial relation shown in their table 2 to correct the proper motions of our sample. Combining radial velocities, distances and proper motions, we calculate the heliocentric space motions (U , V , W) for each star in our sample according to the frame of Johnson & Soderblom (1987). The velocities are in a right-handed coordinate system, with positive U toward the Galactic center, positive V in the direction of Galactic rotation and positive W toward the north Galactic pole. The velocities are corrected for solar motion (10, 5, 7 km s $^{-1}$) (Dehnen & Binney 1998) with respect to the local standard of rest. In order to describe the position of a star in the Galaxy, we transform an equatorial coordinate system to a Galactic coordinate system (l , b), and then transform it to the Galactocentric cylindrical coordinate system (R , θ , Z). The coordinate transformation is performed with the following equations:

$$R = \sqrt{(d \cos b)^2 + R_\odot(R_\odot - 2d \cos b \cos l)},$$

$$\theta = \tan^{-1}\left(\frac{d \cos b \sin l}{R_\odot - d \cos b \cos l}\right),$$

$$Z = Z_\odot + d \sin b,$$

where d is the distance of a star from the Sun, and l and b are Galactic longitude and latitude, respectively. R_\odot and Z_\odot are the positions of the Sun.

To produce a reliable sample, the following criteria are used to select the spectra from the sample. First, high S/N 2MASS photometry is selected, by choosing stars with their Qfl flag equal to AAA, which corresponds to $S/N > 10$. Second, the proper motions with error larger than 10 mas yr $^{-1}$ are excluded. Last, an S/N cut ($S/N \geq 10$) is applied to the sample, leaving the final sample used in the analysis being composed of 71 304 M dwarfs.

Velocity errors of inferred space motions have a strong dependence on radial velocities, proper motions and distances. Our mean proper motion error is 4.1 mas yr $^{-1}$ and mean radial velocity error is ~ 12 km s $^{-1}$. These two uncertainties affect the inferred space velocity components in a complex way and this effect will increase with an increase in the distance to stars. At a distance of 500 pc, a radial velocity error of 12 km s $^{-1}$ and a proper motion error of 4 mas yr $^{-1}$ correspond to a velocity error of ~ 15 km s $^{-1}$. Although the individual velocity may be less reliable because the precision of current proper motions is relatively low, the statistical analysis of the large sample is still of great significance.

4 RESULTS

Here we investigate kinematics and chromospheric activity of M dwarfs in the local Galaxy using our sample derived from LAMOST DR1. The distances to M dwarfs in this sample are less than 900 pc from the solar system. There are few stars later than M5 in the sample, and the distances to these stars are less than 200 pc. The histogram in Figure 2 shows the distribution of vertical distances for M dwarfs from the plane of the Galaxy. Positive values correspond to distances above the plane,

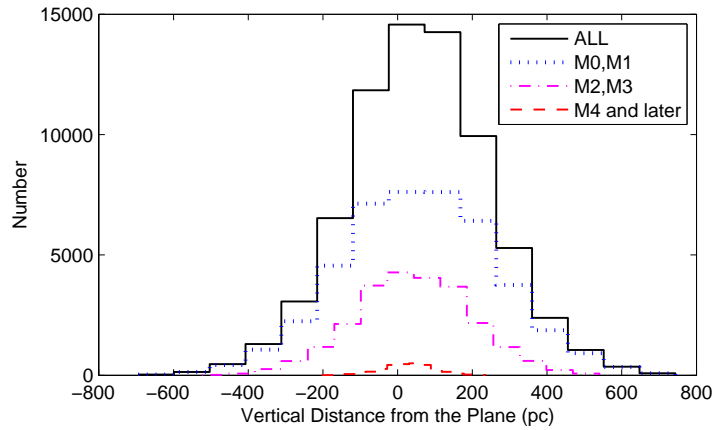


Fig. 2 The distribution of vertical distances for M dwarfs, binned every 100 pc. The solid histogram is the total distribution, while the remaining three histograms represent the distance distribution for three spectral subtype bins as described in the legend.

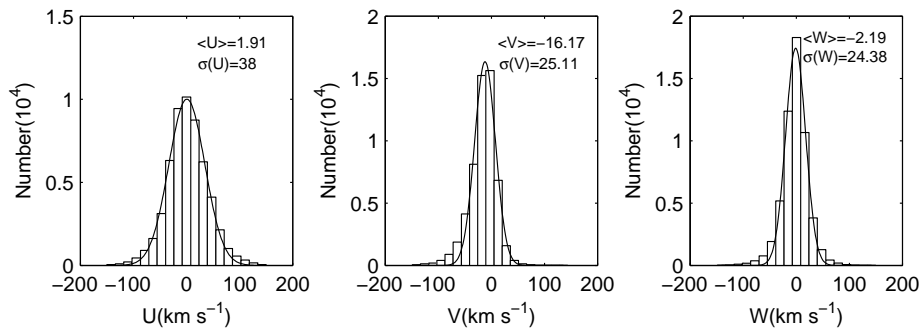


Fig. 3 Histograms of velocities for $\sim 70\,000$ M dwarfs from LAMOST.

while negative values correspond to distances below the plane. The absolute vertical distances of $\sim 90\%$ of stars are within 300 pc.

4.1 Kinematics

Figure 3 shows histograms of the velocities in our sample. The mean and dispersion ($\langle U \rangle$, $\langle V \rangle$, $\langle W \rangle$; $\sigma(U)$, $\sigma(V)$, $\sigma(W)$) of each velocity component are shown as well. The component U covers a larger range than components V and W . Each component can be approximately fitted with a Gaussian curve. The dispersions of velocities are in good agreement with dispersions of M dwarfs at Galactic heights $|z| < 500$ pc in Bochanski et al. (2007). This figure also shows that there are more negative velocities for V , which indicates that most M dwarfs have slow rotation speeds. This conclusion is similar to the results given in previous studies (Bochanski et al. 2007; Allende Prieto 2010).

We further examine the variation of the velocity dispersions with plane height. The sample is binned in 100 pc increments of vertical distance from the Galactic plane. Figure 4 shows the velocity dispersion (left panels) and velocity average (right panels) of U , V and W , from top to bottom

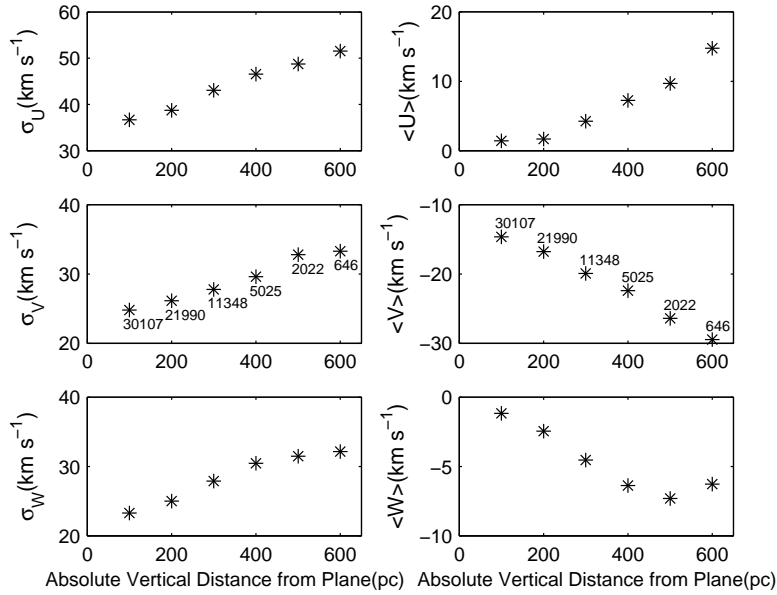


Fig. 4 Velocity dispersion (*left*) and velocity average (*right*) as a function of absolute vertical distance from the Galactic plane in 100 pc wide bins. The number below or above each data point in the middle panels indicates the number of stars in that bin.

respectively. The number of stars in each distance bin is labeled on the middle panel of each column. The left three panels show an apparent increase in the dispersion of U , V and W with the increase in absolute vertical distance from the plane. The right panels show that $\langle U \rangle$ increases towards its positive direction, $\langle V \rangle$ increases towards its negative direction with Galactic height and $\langle W \rangle$ is in a narrow range and does not show a monotonic change. Though the general trends agree well with the trends of the thin disk shown in Bochanski et al. (2007), there is a disagreement in $\langle W \rangle$. A possible reason is that the value of $\langle W \rangle$ is relatively small in a narrow range near 0 km s^{-1} and it may be sensitive to systematic errors in the proper motions.

4.2 Chromospheric Activity

The $H\alpha$ emission line is produced by collisional excitation in the chromospheres of M dwarfs, and it is the strongest indicator of magnetic activity in late-type stars (West et al. 2004). The activity strength is often measured by the ratio of the luminosity in $H\alpha$ to the bolometric luminosity ($L_{H\alpha}/L_{\text{bol}}$) (Hawley et al. 1996). Here we do not measure the activity strength but use the $H\alpha$ emission line as a rough indicator that can reveal whether a star is active. Using the magnetic activity criteria described in Yi et al. (2014), we investigate the magnetic activity fraction of stars in our sample as a function of spectral type. The criteria judge a star to be active if there exists an obvious $H\alpha$ emission line in its spectrum (see the detailed description of the magnetic activity criteria in Yi et al. 2014). Using the criteria, 5649 of the stars in our sample are $H\alpha$ active while 35 952 are $H\alpha$ inactive. The activity fractions of M0–M5 are listed in Table 1, which indicates that later-subtype M dwarfs have a higher activity fraction. The activity fraction of M6–M9 was not provided here because the number of late-type M dwarfs is too small to produce a reasonable activity fraction.

Table 1 $H\alpha$ Activity Fraction for Each Subtype

SPT	Active	Inactive	Activity fraction (%)
M0	745	16432	4.34
M1	1108	10744	9.35
M2	1342	6036	18.19
M3	1386	2257	38.05
M4	890	457	66.07
M5	178	26	87.25

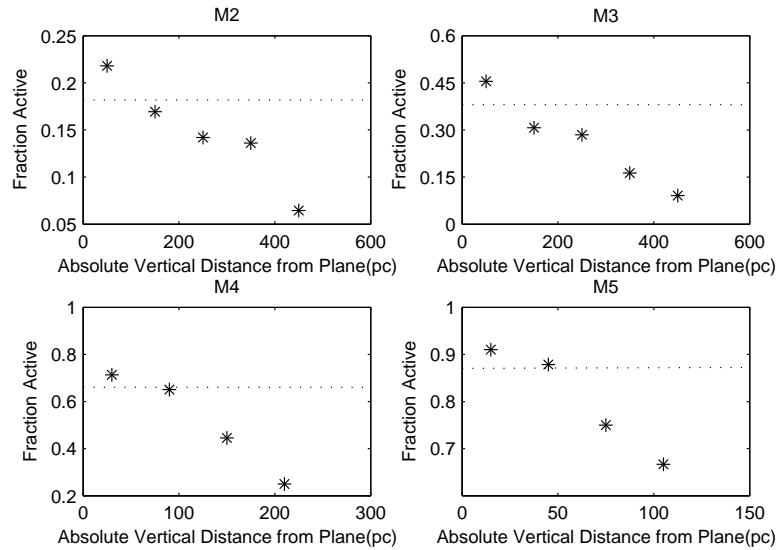


Fig. 5 $H\alpha$ activity fractions as a function of absolute vertical distance from the Galactic plane for M2–M5. The dotted line in each panel plots the general activity fraction level, which corresponds to values shown in Table 1.

As the activity fraction is highly dependent on the location of the stars in the Galaxy (West et al. 2008), we examine the activity correlation with Galactic height. Figure 5 shows $H\alpha$ activity fractions for M2–M5 as a function of absolute vertical distance from the Galactic plane. Spectral types earlier than M2 and later than M5 were not included due to an insufficient sample of active stars. As shown in Figure 5, the magnetic activity fraction decreases with the Galactic plane height, which is in agreement with the age–activity relationship in previous studies (West et al. 2008, 2011). This indicates that M dwarfs closer to the Galactic plane are more likely to be active stars. Together with the theory that the stellar chromospheric activity levels will become weaker over time (Soderblom et al. 1991), we can infer that the M dwarfs closer to the Galactic plane are younger, which is consistent with the current model of the Galaxy.

4.3 Differences between the Thin and Thick Disks

It has been revealed that the Galactic disk contains a thin disk and a thick disk, and these two stellar populations have different kinematic properties and different mean metallicities. The thick disk stars move in a scale height of 800 pc (Reylé & Robin 2001) to 1300 pc (Chen 1997), while the thin disk has a scale height of 100 pc to 300 pc (Gilmore & Reid 1983; Robin et al. 1996). An investigation of

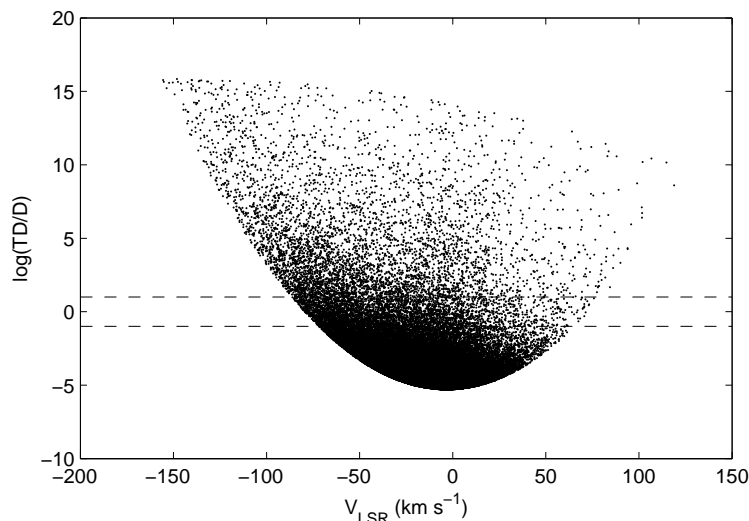


Fig. 6 The TD/D relative probabilities. Dashed lines indicate $TD/D = 10$ (*upper*) and $TD/D = 0.1$ (*lower*). The points above the line $TD/D = 10$ correspond to thick disk stars, while points below the line $TD/D = 0.1$ correspond to thin disk stars.

the densities of the stellar populations in the solar neighborhood gives a thick disk fraction of 2%–15% (Gilmore & Reid 1983; Chen 1997; Chen et al. 2001; Soubiran et al. 2003), and the value is around 6% given by Robin et al. (1996) and Buser et al. (1999). According to these previous results, our sample should include a portion of thick disk stars. Therefore, we select thick disk stars and thin disk stars from our sample to examine differences in properties between these two populations.

We take a pure kinematical approach to separate our stars using the method of Bensby et al. (2003). This technique computes the probability of stars belonging to a population by taking into account their space motion, together with the observed fraction of stars for the population in the solar neighborhood. Applying this method to our sample, we derive 56 243 stars belonging to the thin disk and 4096 stars belonging to the thick disk.

Figure 6 shows the relative probability distribution of all the stars in our sample. Stars with relative probabilities $TD/D \geq 10$ are selected as thick disk stars, while stars with relative probabilities $TD/D \leq 0.1$ are selected as thin disk stars. The stars with relative probabilities between 0.1 and 10 are not selected into any group to minimize the mutual contamination.

4.3.1 Metallicity

We try to investigate the difference in metallicity between thick disk stars and thin disk stars through certain molecular band indices which are sensitive to metallicity. It is known that indices of CaH2, CaH3 and TiO5 are relevant to metallicity and have been used to roughly discriminate subdwarfs from stars with solar metallicity (Reid et al. 1995). We plot the ratio $(\text{CaH2} + \text{CaH3})/\text{TiO5}$ as a function of spectral type, as shown in Figure 7. However, there are no significant ratio differences between the thin and thick disks, a similar result to what was also shown in Bochanski et al. (2007). This implies that the ratio of $(\text{CaH2} + \text{CaH3})/\text{TiO5}$ may not be a good proxy of metallicity. We thus examine the metallicity indicator ζ instead. We compute ζ following the latest definition described in Lépine et al. (2013).

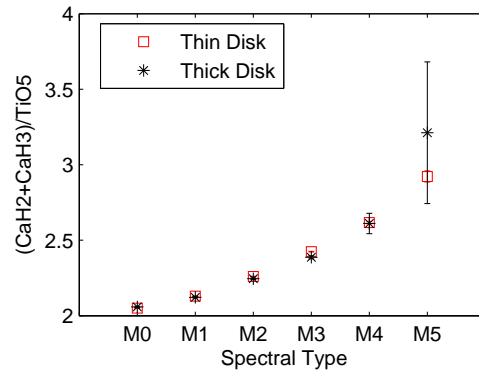


Fig. 7 $(\text{CaH}_2+\text{CaH}_3)/\text{TiO}_5$ vs. spectral type for the thin disk (*open squares*) and thick disk (*stars*) populations.

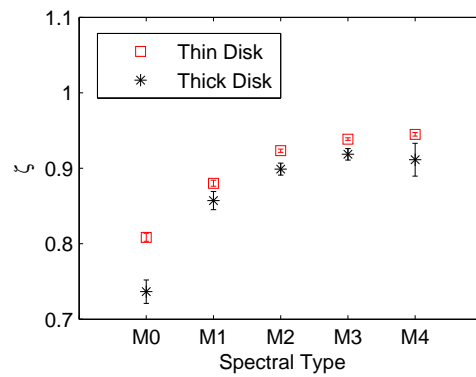


Fig. 8 Metal-sensitive parameter ζ vs. spectral type for the thin disk (*open squares*) and thick disk (*stars*) populations. A higher ζ indicates a higher metallicity (Lépine et al. 2003).

Figure 8 shows the difference in ζ between thin disk stars and thick disk stars at a given spectral type. ζ of the thick disk population is smaller than that of the thin disk population at a given spectral type, which indicates that the thick disk has lower metallicity than the thin disk. This result offers evidence that mean metallicity of the thick disk is lower than that of the thin disk, as suggested in previous studies (Bensby et al. 2003; Reid & Majewski 1993; Chiba & Beers 2000).

4.3.2 Chromospheric activity

To study the difference in $H\alpha$ activity between the thin disk and thick disk populations, we compute their corresponding activity fraction. The $H\alpha$ activity fraction as a function of spectral type for the thin and thick disk populations is shown in Figure 9. According to the previous result that magnetic activity in M dwarfs decreases with age (West et al. 2008), a population composed of older M dwarfs should possess a lower activity fraction. Just as we expected, in this figure activity fractions of the thick disk are smaller than those of the thin disk. This result demonstrates that the thick disk is an older system.

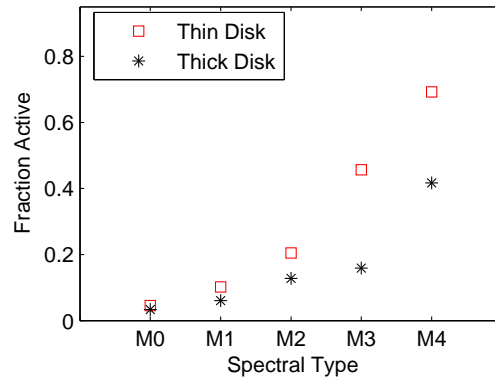


Fig. 9 $H\alpha$ activity fractions as a function of spectral type for the thin disk (*open squares*) and thick disk (*stars*) populations.

5 CONCLUSIONS

Using 71 304 spectra of M dwarfs from LAMOST DR1 together with photometry from the 2MASS catalog and proper motions from the PPMXL catalog, we have computed the space motions and the Galactocentric cylindrical coordinates for these M dwarfs. We have examined the kinematic properties and chromospheric activities of this sample. The velocity dispersion of the stars in our sample is (38, 25, 24 km s⁻¹) for (U , V , W). Our investigation indicates that the velocity dispersion of (U , V , W) increases with the absolute vertical distance from the plane. Our examination on the chromospheric activities of stars shows that the magnetic activity fraction decreases with height from the Galactic plane, which indicates M dwarfs closer to the Galactic plane are more active. Finally, thin disk stars and thick disk stars are selected to examine differences in the properties between the thin disk population and the thick disk population. The activity fraction of the thin disk at a given spectral type is higher than that of the thick disk, while the metallicity investigation confirms that the thin disk possesses higher metallicity than the thick disk. During the metallicity investigation of the two populations, we find that the metallicity indicator ζ is more effective than the ratio of (CaH2+CaH3)/TiO5 in identifying differences in metallicity between the two populations. The investigation demonstrates that the selected thin and thick disk populations are distinct in terms of their chromospheric activities and metallicity. To sum up, using the data from LAMOST DR1, we get some conclusions that are consistent with previous studies and provide a better understanding of the structure of the Galactic disk. However, there are larger uncertainties in proper motions and distances which impair the ability to conduct a deeper exploration of M dwarf kinematics. A more thorough investigation on M dwarf kinematics requires more accurate proper motions and distances which may be provided by the *Gaia* mission (Lindgren & Perryman 1996).

Acknowledgements This work was supported by the National Natural Science Foundation of China (Grant Nos. 11390371, 11233004, 11303061 and U1431106). The Guo Shou Jing Telescope (the Large Sky Area Multi-Object Fiber Spectroscopic Telescope, LAMOST) is a National Major Scientific Project built by the Chinese Academy of Sciences. Funding for the project has been provided by the National Development and Reform Commission. LAMOST is operated and managed by the National Astronomical Observatories, Chinese Academy of Sciences.

References

- Allende Prieto, C. 2010, in IAU Symposium, 265, eds. K. Cunha, M. Spite, & B. Barbuy, 304
- Bensby, T., Feltzing, S., & Lundström, I. 2003, *A&A*, 410, 527
- Bessell, M. S., & Brett, J. M. 1988, *PASP*, 100, 1134
- Bochanski, J. J., Hawley, S. L., Reid, I. N., et al. 2005, *AJ*, 130, 1871
- Bochanski, J. J., Munn, J. A., Hawley, S. L., et al. 2007, *AJ*, 134, 2418
- Buser, R., Rong, J., & Karaali, S. 1999, *A&A*, 348, 98
- Carlin, J. L., DeLaunay, J., Newberg, H. J., et al. 2013, *ApJ*, 777, L5
- Chen, B. 1997, *ApJ*, 491, 181
- Chen, B.-Q., Liu, X.-W., Yuan, H.-B., et al. 2014, *MNRAS*, 443, 1192
- Chen, B., Stoughton, C., Smith, J. A., et al. 2001, *ApJ*, 553, 184
- Chiba, M., & Beers, T. C. 2000, *AJ*, 119, 2843
- Covey, K. R., Ivezić, Ž., Schlegel, D., et al. 2007, *AJ*, 134, 2398
- Cui, X.-Q., Zhao, Y.-H., Chu, Y.-Q., et al. 2012, *RAA (Research in Astronomy and Astrophysics)*, 12, 1197
- Dehnen, W., & Binney, J. J. 1998, *MNRAS*, 298, 387
- Gilmore, G., & Reid, N. 1983, *MNRAS*, 202, 1025
- Gizis, J. E., Reid, I. N., & Hawley, S. L. 2002, *AJ*, 123, 3356
- Hawley, S. L., Gizis, J. E., & Reid, I. N. 1996, *AJ*, 112, 2799
- Hawley, S. L., Covey, K. R., Knapp, G. R., et al. 2002, *AJ*, 123, 3409
- Johnson, D. R. H., & Soderblom, D. R. 1987, *AJ*, 93, 864
- Lépine, S., Hilton, E. J., Mann, A. W., et al. 2013, *AJ*, 145, 102
- Lépine, S., Rich, R. M., & Shara, M. M. 2003, *AJ*, 125, 1598
- Lindegren, L., & Perryman, M. A. C. 1996, *A&AS*, 116, 579
- Luo, A.-L., Zhang, H.-T., Zhao, Y.-H., et al. 2012, *RAA (Research in Astronomy and Astrophysics)*, 12, 1243
- Ratnatunga, K. U., & Uggren, A. R. 1997, *ApJ*, 476, 811
- Reid, I. N., Gizis, J. E., & Hawley, S. L. 2002, *AJ*, 124, 2721
- Reid, I. N., Hawley, S. L., & Gizis, J. E. 1995, *AJ*, 110, 1838
- Reid, N., & Majewski, S. R. 1993, *ApJ*, 409, 635
- Reylé, C., & Robin, A. C. 2001, *A&A*, 373, 886
- Robin, A. C., Haywood, M., Creze, M., Ojha, D. K., & Bienayme, O. 1996, *A&A*, 305, 125
- Roeser, S., Demleitner, M., & Schilbach, E. 2010, *AJ*, 139, 2440
- Schlafly, E. F., & Finkbeiner, D. P. 2011, *ApJ*, 737, 103
- Schlegel, D. J., Finkbeiner, D. P., & Davis, M. 1998, *ApJ*, 500, 525
- Skrutskie, M. F., Cutri, R. M., Stiening, R., et al. 2006, *AJ*, 131, 1163
- Soderblom, D. R., Duncan, D. K., & Johnson, D. R. H. 1991, *ApJ*, 375, 722
- Soubiran, C., Bienaymé, O., & Siebert, A. 2003, *A&A*, 398, 141
- Vysotsky, A. N. 1956, *AJ*, 61, 201
- West, A. A., Hawley, S. L., Bochanski, J. J., et al. 2008, *AJ*, 135, 785
- West, A. A., Hawley, S. L., Walkowicz, L. M., et al. 2004, *AJ*, 128, 426
- West, A. A., Morgan, D. P., Bochanski, J. J., et al. 2011, *AJ*, 141, 97
- Wielen, R. 1977, *A&A*, 60, 263
- Yi, Z., Luo, A., Song, Y., et al. 2014, *AJ*, 147, 33
- York, D. G., Adelman, J., Anderson, Jr., J. E., et al. 2000, *AJ*, 120, 1579
- Zhao, G., Zhao, Y.-H., Chu, Y.-Q., Jing, Y.-P., & Deng, L.-C. 2012, *RAA (Research in Astronomy and Astrophysics)*, 12, 723